Optimizing Secure Data Transmission in 6G-Enabled IoMT Using Blockchain Integration

Aruna Malik⬦, Vikas Tyagi, Samayveer Singh⬦, *Senior Member, IEEE*, Rajeev Kumar⬦, Huaming Wu⬦, *Senior Member, IEEE*, and Sukhpal Singh Gill⬦

Abstract—The advent of sixth-generation (6G) technology is poised to revolutionize connectivity, particularly by enhancing the integration of Internet of Medical Things (IoMT) devices. This advancement offers ultra-fast data transmission, low latency, and high mobility but also brings the challenge of ensuring secure and energy-efficient communication. To solve these challenges, this paper introduces a novel hybrid greylag goose-based optimized clustering (HGGOC) algorithm. It merges the efficiency of greylag goose optimization with the precision of the golden sine strategy. The Lévy flight mechanism guides the algorithm to optimize cluster head selection in 6G-enabled IoMT networks. The integration of blockchain technology further strengthens data security and transparency. Simulation results show that HGGOC surpasses existing methods, delivering up to 64% improvement in network stability, a 47% increase in node lifetime, and a 59% boost in energy efficiency and data throughput. These findings position HGGOC as a promising solution for sustainable communication in 6G-enabled IoMT environments.

Index Terms—Internet of Medical Things, blockchain, data dissemination, energy efficiency, sustainable communication.

I. INTRODUCTION

IN RECENT years, advancements in sensing technologies have underscored the growing need for reliable deployment and integration of Internet of Medical Things (IoMT) devices. As these devices become more prevalent, modern communication technologies, particularly wireless networks, have become the backbone for connecting IoMT systems [1]. However, despite the adoption of fifth-generation (5G) and beyond-5G technologies to support these networks, they face significant challenges such as limited data rates and insufficient capacity.

Aruna Malik, Vikas Tyagi, and Samayveer Singh are with the Department of Computer Science and Engineering, National Institute of Technology Jalandhar, Jalandhar 144008, India (e-mail: malika@nitj.ac.in; vikast.cs.19@nitj.ac.in; samays@nitj.ac.in).

Rajeev Kumar is with the Department of Computer Science and Engineering, Delhi Technological University, New Delhi 110042, India (e-mail: rajeevkumar@dtu.ac.in).

Huaming Wu is with the Center for Applied Mathematics, Tianjin University, Tianjin 300072, China (e-mail: whming@tju.edu.cn).

Sukhpal Singh Gill is with the School of Electronic Engineering and Computer Science, Queen Mary University of London, E1 4NS London, U.K. (e-mail: s.s.gill@qmul.ac.uk).

These limitations make it difficult to handle advanced applications like holographic communications. These limitations have spurred growing interest in the development of sixth-generation (6G) technology, which promises to address these shortcomings and offer enhanced capabilities [2].

6G technology is characterized by its potential for ultra-high data rates and minimal end-to-end delays, which are essential for a wide range of applications, including forest fire detection, IoMT, and intelligent transportation systems [3]. These diverse applications form a triangular coverage model, illustrating the vast utility of 6G technology in smart city scenarios [4]. However, a significant challenge with 6G and IoMT devices lies in their high energy consumption and limited battery life, which can impede their ability to maintain intelligent and seamless connectivity [5]. This situation necessitates the development of energy-efficient, or sustainable communication strategies for managing the connectivity of a vast array of 6G-enabled IoMT devices. Nevertheless, many key challenges exist: In large-scale IoMT networks, managing energy consumption is crucial due to the limited battery power of numerous devices, necessitating energy-efficient communication protocols like the one proposed in our work. Additionally, ensuring the security and integrity of medical data is a significant challenge, particularly due to the decentralized nature of IoMT devices, which we address through blockchain integration [6]. As these networks grow, scalability becomes increasingly complex, requiring efficient management of cluster head selection, network stability, and reliable data transmission. Moreover, in healthcare applications, maintaining low latency while ensuring energy efficiency and security presents a critical technical challenge [7]. In addressing these challenges, our work focuses on optimizing the cluster head (CH) selection process for cluster-based routing in IoMT networks. The existing research, such as [8], [9], [10], [11] have explored various methods like genetic algorithms for CH selection. These studies highlight the importance of a metaheuristic approach in optimizing CH selection. Additionally, strategies like the use of multiple data-collecting sinks [12], [13], [14], can reduce the load on relay nodes.

To advance this field, the proposed work introduces a novel approach that combines the exploratory aspects of the greylag goose-based optimized clustering (GGOC). It also incorporates the exploitation capabilities of the golden sine strategy guided by the Lévy flight mechanism. The motivation behind this unique combination of proposed hybrid greylag

goose-based optimized clustering (HGGOC) is deeply rooted in addressing the ever-growing challenges of data dissemination in 6G-enabled IoMT networks. In these networks, the pursuit of excellence is intricately intertwined with the imperatives of energy efficiency and cost-effectiveness. The proposed HGGOC, inspired by the greylag geese's remarkable navigational capabilities, epitomizes optimization exploration. We aim to explore uncharted territories within the vast data space by harnessing these geese's inherent curiosity and adaptability, seeking optimal solutions that traditional methods might overlook. This exploration element is vital in ensuring that our approach is not confined to local optima but embraces the full spectrum of possibilities, thereby enhancing the robustness and adaptability of our optimization strategy. Complementing the GGOC, the golden sine strategy guided by the Lévy flight mechanism brings a sophisticated level of exploitation to our hybrid approach. Inspired by the harmonic nature of the golden ratio, the golden sine strategy imbues our optimization with precision and efficiency. Coupled with the Lévy flight mechanism, which introduces stochasticity and long-range jumps, our strategy balances thorough exploration and targeted exploitation. This dynamic interplay ensures that our optimization adapts to the evolving nature of data dissemination challenges, optimizing resource utilization and network performance. The 6G-enabled IoMT networks prioritize security and privacy alongside optimization strategies. The proposed HGGOC approach integrates blockchain technology to enhance data dissemination in these networks. Blockchain's decentralized and tamper-resistant nature ensures secure and transparent data management, reducing vulnerabilities and enabling accountable network operations. This work focuses on advancing green communication in 6G-enabled massive IoMT networks. The main contributions of this paper are outlined as follows:

- We propose a cluster-based routing method for data dissemination that incorporates a novel hybrid metaheuristic technique, the Greylag Goose-based Optimized Clustering (HGGOC) algorithm. This technique combines elements of the Greylag Goose Optimization (GGO) algorithm with the golden sine strategy, guided by the Lévy flight mechanism, to enhance the selection of cluster heads (CHs) within the network. The main contributions of this work are the reduction of energy consumption and the extension of the lifespan of 6G-enabled IoMT devices.
- We develop a fitness function for the proposed HGGOC that considers multiple factors for CH selection. These factors include residual energy, node and sink proximity, remaining energy levels of 6G-enabled IoMT devices, and cluster energy. This multifaceted approach ensures a more comprehensive and efficient CH selection process.
- Integrating blockchain technology with 6G-enabled IoMT systems significantly enhances security and privacy. This integration capitalizes on blockchain's robust features to provide secure and transparent data management across widespread IoMT networks for data dissemination.
- We compared its simulation results with those of recent cluster-based routing methods, including ICITS [8], OptiGA-ASR-DDC [9],

OptimizedGA-MS-In&Out-DDC-ASR [12], and OptiGeA-MoMS-In&Out-DDC [14]. Our findings demonstrate that the proposed HGGOC method outperforms these existing approaches regarding efficiency and effectiveness in 6G-enabled IoMT networks.

The structure of this paper is as follows: Section II reviews related studies. Section III describes the network model assumptions. Section IV details the proposed hybrid clustering approach and its fitness evaluation. Section V demonstrates how blockchain technology is integrated into the proposed work. Section VI presents the results and compares them with state-of-the-art techniques. Finally, Section VII concludes this paper and suggests directions for future research.

II. RELATED WORK

A key feature of 6G is its utilization of terahertz frequency bands, which promise to offer significantly higher bandwidth up to three times greater than that of 5G. Recent research has extensively explored the core technologies and components associated with 6G. A recurring theme in these studies concerns energy consumption, which significantly limits the capabilities of 6G-enabled IoMT devices. This challenge highlights the urgent need for optimized solutions to enhance energy efficiency.

Pokhrel et al. [1] introduced a cluster-based intelligent routing protocol that employs multiple gateways to alleviate network hotspot problems. Verma et al. [8] developed intelligent and secure clustering in wireless sensor network (WSN)-based intelligent transportation systems. They utilized a hybrid optimization method called GABAT that integrates the strengths of genetic algorithm (GA) and BAT algorithm (BA), to reduce the distance data must travel. However, GABAT introduces higher overhead and complexity when managing large-scale sensor networks. Singh et al. [9] introduced a dynamic data transmission method for communicable diseases in IoMT environments, leveraging a GA. Their method optimizes energy usage in IoMT devices by employing GA-based evolutionary processing that adapts to the dynamic range of sensors. It also includes a defined deployment area for IoMT devices to address energy depletion issues, incorporates multiple sinks, and utilizes a direct data collection strategy. While this approach enhances system performance and reduces extensive data packet movement, GA still suffers from slower convergence.

Nandan et al. [12] presented a green data collection and transmission method for IoT-based WSNs utilizing an optimized GA. This approach focuses on reducing intra-cluster distances, efficiently using node energy, and minimizing hop counts. It also included direct data transmission with movable sinks to lessen communication distances and hotspot issues, and a dynamic sensing range to decrease CH sensing range overlap and save transmission energy. Singh et al. [14] introduced a secure and energy-efficient system focusing on communicable diseases. Enhanced by a genetic algorithm, this system utilizes a WSN with OptiGeA protocol, designed specifically for IoT-enabled WSNs in healthcare. OptiGeA optimizes CH selection by considering node energy, density,

TABLE I
SUMMARY OF STATE-OF-THE-ART CLUSTER-BASED ROUTING APPROACHES FOR ENERGY-EFFICIENT WSNS

Research	Protocol	Methodology	Advantages	Research Gaps
Sahoo *et al.* [15]	PSO-based energy efficient clustering & sink mobility (PSO-ECSM)	Particle swarm optimization & mobile sink approach	Stability & prolonged network lifetime	Reducing end-to-end delay using a hybrid routing method
Alghamdi *et al.* [16]	Energy efficient protocol for optimized CH selection	Dragonfly & Firefly algorithm	Improved statistics for node longevity, network convergence & energy consumption	Achieving a balance between computational cost in the algorithms & calculations for further exploration
Prakash *et al.* [17]	Energy-optimization route & cluster head selection	M-PSO & GA	Used probability to select CHs & GA for optimal path	Re-clustering challenges need more investigation
Osamy *et al.* [18]	Load-balancing aware clustering Scheme (LBACS)	Graph theory concepts	Designed clusters with load balancing	Maintain load balancing, data flow & connectivity under changing network conditions
Loganathan *et al.* [19]	Load-balanced clustering for energy-aware routing (LBCE-EAR)	Clusters are formed as concentric circles	Cluster diameters are measured	Load balancing is achieved to maintain energy efficiency
Prasad *et al.* [20]	BAT algorithm	Barabasi−Albert (BA) model & Topsis (T) technique	Reduced intracluster & intercluster distances by retaining best performance attachments	Only varying the cluster size considered to achieve load balancing
Verma *et al.* [8]	Intelligent Clustering approach for ITS (IC-ITS)	Hybrid optimization of GA and BAT	Ensures energy efficiency & load balancing	Only CH rotation strategy considered for load balancing
Singh *et al.* [9]	Optimized data aggregation algorithm	GA	Improves data aggregation & reduces energy consumption	All direct information requires multiple paths & fixed topologies
Nandan *et al.* [12]	Optimized GA-based data collection method	GA	Improves intracluster efficiency & reduces hop count	Movable sink strategies

distance, and capacity. However, the cost of the implication and complexity is high. Sahoo et al. explored the optimization of sink mobility with their particle swarm optimization-based energy-efficient clustering based on sink mobility (PSO-ECSM), but this led to increased overhead due to the moving sink [15]. In another approach, Ali et al. integrated novel rank-based clustering (NRC) with their ARSH-FATI-based cluster-head (CH) selection method, aiming to reduce energy consumption [21]. It involves significant computational complexity. Behera et al. [22] proposed an improved residual energy selection (I-RES) approach, focused solely on residual energy for CH selection, leaving room for further improvement. It focuses solely on residual energy for cluster-head selection, which may lead to suboptimal network performance as other important factors like node density, distance, and communication overhead are not considered in the selection process. Tariq et al. discussed an energy-efficient routing protocol for improving the link quality [23]. This approach introduces computational overhead and increased complexity in dynamic, large-scale IoT environments. Table I shows the summary of state-of-the-art cluster-based routing approaches for energy-efficient WSNs.

III. SYSTEM MODEL

In this study, 6G-enabled IoMT devices are deployed in the monitoring scenarios by varying initial energy levels among 6G-enabled IoMT devices. The network is composed of N 6G-enabled IoMT devices with three levels of energy heterogeneity. The network includes a mix of advanced, intermediate, and normal 6G-enabled IoMT devices with each type characterized by distinct initial energy levels. The advanced 6G-enabled IoMT devices have higher initial energy than intermediate 6G-enabled IoMT devices, and both have more energy than normal nodes, following the energy inequality $E_{nrm} < E_{int} < E_{adv}$. The total number of each type of 6G-enabled IoMT devices is advanced (n_{adv}), intermediate (n_{int}), and normal (n_{nrm}) reflects a descending order, with normal 6G-enabled IoMT devices being the most numerous, satisfying the inequality $n_{nrm} > n_{int} > n_{adv}$. The initial energy for each 6G-enabled IoMT device type is denoted as E_0, and the total energy in the network is represented by E_t. The advanced 6G-enabled IoMT devices have their energy defined

as $E_0 \times (1 + \omega) \times n_{adv}$, and intermediate 6G-enabled IoMT devices as $E_0 \times (1 + \Psi) \times n_{int}$, with normal 6G-enabled IoMT devices at $E_0 \times n_{nrm}$. Thus, the total energy for the network is the sum of the energies of advanced, intermediate, and normal 6G-enabled IoMT devices, resulting in $E_T = E_{adv} + E_{int} + E_{nrm}$. The total energy is $E_T = E_0 \times N \times (1 + \Psi \times k_o + k \times \omega)$, combining the energy contributions from all levels. The energy ratios Ψ and ω correspond to the energy fractions of advanced and intermediate 6G-enabled IoMT devices, respectively. The proportions of advanced and intermediate 6G-enabled IoMT devices within the network are indicated by k and k_o. There are several assumptions about the network setup of the proposed work which are outlined as follows:

- The proposed work assumes a static network configuration, despite the capability of 6G's to support high mobility in IoMT devices. Both the data-collecting sink and the 6G-enabled IoMT devices are considered stationary throughout the network operation.
- It is assumed that all 6G-enabled IoMT devices in the network have uniform configurations and operational characteristics, though nodes possess heterogeneous energy capabilities. This assumption simplifies the analysis and implementation of the proposed method.
- The data-collecting sink is assumed to operate without energy limitations, in contrast to the IoMT devices, which are subject to energy constraints.
- The IoMT devices in the network are assumed to be wireless sensor nodes equipped with 6G communication capabilities, enhancing their connectivity and data transmission efficiency.

In this work, we considered the same radio energy consumption model for transmitting and receiving data between the 6G-enabled IoMT devices and sinks as discussed in the existing works [8], [9], [12], [14]. Fig. 1 illustrates a secure data transmission framework in a 6G-enabled Internet of Medical Things (IoMT) network using blockchain technology. The framework consists of three parts: the 6G-enabled IoMT network, the blockchain network, and the administrator domain. The 6G-enabled IoMT network includes devices in homes, hospitals, and ambulances, leveraging 6G technology for fast, low-latency communication. The blockchain network ensures secure and transparent data management through smart contracts, making the data unalterable and traceable.
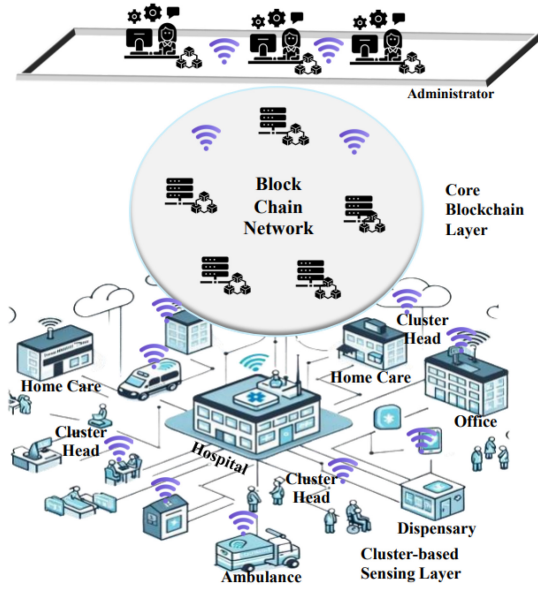
Fig. 1. Secure framework for a 6G-Enabled IoMT network.

The administrator domain oversees the network, managing its operation and addressing any issues. Data flows from IoMT devices to a sink, which collects and sends the data to the blockchain for secure storage and processing. The administrator ensures the system operates smoothly, monitors the network, and ensures adherence to policies.

IV. PROPOSED HYBRID GREYLAG GOOSE-BASED OPTIMIZED CLUSTERING (HGGOC)

The optimized clustering method, inspired by the greylag goose, initiates by generating a diverse set of individuals through a stochastic process. Each individual proposes a potential solution that is subject to evaluation for potential inclusion in the pool of solutions to address the problem. The dynamic group behavior of the native GGO algorithm [24] assigns each member to either an exploration or an exploitation group. Throughout each iteration, the quantity of potential solutions in each group is dynamically adjusted based on the solution identified as the most optimal. The goose explorer embarks on a journey to investigate novel locations proximate to its current position. The responsibility for refining the existing solutions lies with the exploitation team. After each cycle, the GGO evaluates participants to identify those who have achieved the highest fitness level and duly acknowledges their accomplishments. The following steps elaborate on the exploration and exploitation phases in intricate detail.

A. Exploration Phase: Migration

This process involves the goose explorer actively searching for promising and unexplored locations near its current position. The explorer iteratively evaluates various potential options in the vicinity to identify the most suitable one based on its fitness. The proposed algorithm utilizes the following equations to compute the updated position of the agent ($X_P(I+$

1)), by adjusting the auxiliary vectors Aux_v and CX_v. The updated position of the agent is represented as follows:

$$X_P(I+1) = X_P^*(I) - Aux_v \cdot |CX_v \cdot (X_P^*(I) - X_P(I))|, \quad (1)$$

where $X_P(I)$ signifies an agent from the population at the Ith iteration, and $X_P^*(I)$ denotes the position of the best solution (leader). Specifically, $Aux_v = 2\alpha R_{nd1} - \alpha$ and $CX_v = 2R_{nd2}$ during iterations, where α linearly decreases from 2 to 0 throughout the iterations. The values of R_{nd1} and R_{nd2} experience random variations within the range [0, 1].

To foster diversity and enhance exploration, Eq. (2) is employed, involving the selection of three random search agents (paddlings denoted with (Pdl)) named X_P^{Pdl1}, X_P^{Pdl2}, and X_P^{Pdl3}. This approach ensures that agents are not excessively influenced by a single leader position, promoting more extensive exploration. Subsequently, the current search agent's position update is determined below when $|Aux_v| \geq 1$.

$$X_P(I+1) = F_{w1} * X_P^{Pdl1} + F_{w2} * S * \left(X_P^{Pdl2} - X_P^{Pdl3}\right)$$
$$+ F_{w3} * (1 - S) * \left(X_P(I) - X_P^{Pdl1}\right), \quad (2)$$

where F_{w1}, F_{w2}, and F_{w3} denote the weight factors associated with each paddling. These weight factors vary within the interval [0, 2]. The parameter S experiences an exponential decrease, and its calculation is defined by:

$$S = 1 - \frac{I}{I_{Max}}, \quad (3)$$

where I_{Max} denotes the maximum number of iterations. The second updating procedure, which includes diminishing both α and Aux_v vector values, is applied when $R_{nd3} \geq 0.5$.

$$X_P(I+1) = F_{w4} \cdot |X_P^*(I) - X_P(I)| \cdot e^{bl} \cos(2\pi l)$$
$$+ [2 \cdot F_{w1} \cdot (R_{nd4} + R_{nd5})] * X_P^*(I), \quad (4)$$

where the constant parameter b remains unchanged, and l denotes a random value within the range $[-1, 1]$. F_{w4} varies within the interval [0, 2], while the random variables, R_{nd4} and R_{nd5}, undergo updates within the range [0, 1].

B. Exploitation Phase: Attacking

The exploitation team is responsible for refining the current solutions. At the end of each cycle, the proposed HGGOC algorithm identifies individuals with the highest fitness and recognizes their contributions. To achieve its exploitation goals, the algorithm employs two distinct strategies, as outlined below.

1) Progressing Toward the Optimal Solution: The motion of three solutions (sentries denoted as (sty), specifically X_P^{sty1}, X_P^{sty2}, and X_P^{sty3}, serves as guidance for other individuals $(X_P^{(non\_sty)})$ to adjust their positions towards the estimated location of the prey. The process of updating positions is illustrated as follows:

$$X_{P1} = X_P^{sty1} - Aux_v \cdot |CX_v \cdot X_P^{sty1} - X_P(I)|, \quad (5)$$
$$X_{P2} = X_P^{sty2} - Aux_v \cdot |CX_v \cdot X_P^{sty2} - X_P(I)|, \quad (6)$$
$$X_{P3} = X_P^{sty3} - Aux_v \cdot |CX_v \cdot X_P^{sty3} - X_P(I)|. \quad (7)$$

The updated positions for the population $X_P(I + 1)$ can be described as the mean of the three solutions:

$$X_P(I + 1) = \frac{X_{P1} + X_{P2} + X_{P3}}{3}. \tag{8}$$

2) Exploring the Vicinity of the Optimal Solution: It involves identifying the most promising option situated near the best response (leader) during flight. Consequently, certain individuals undertake a search for improvements by examining areas close to the optimal response, denoted as PX_{flock}. The mathematical formulation of this process is represented by:

$$X_P(I + 1) = X_P(I) + F_{w1}(1 - S)CX_v\Big(X_P(I) - X_P^{\text{flock}}\Big), \tag{9}$$

which encompasses identifying the most favorable choice located in proximity to the optimal response (leader) during flight. As a result, specific individuals engage in a quest for enhancements by scrutinizing areas close to the optimal response, indicated as X_P^{flock}.

C. The Lévy Flight Mechanism With Golden Sine Strategy

In the optimization phase of the standard native GGO algorithm, geese determine their attack position based on a fixed behavioral track post-migration. However, the inherent singularity of the action model causes geese to persistently fly in a set angle and direction during movement. Consequently, this leads to a failure in locating the optimal position, and the elevated population density significantly hampers the ability to break free from local extreme values. To address this issue, a later stage of the algorithm incorporates the golden sine strategy guided by the Lévy flight mechanism [25]. The proposed HGGOC introduces the capability to traverse all values of the sine function (all points on the identity element) by leveraging the relationship between the sine function and the unit circle. During this process, including the golden section number serves to narrow the search space and guide seagull individuals toward the optimal solution.

Simultaneously, the Lévy flight mechanism is introduced to provide guidance. By incorporating uncertainty into both the direction and step size of the Lévy flight, the algorithm disrupts the population's positions, expands the search range, and enhances its ability to escape local extrema. The mathematical model of Lévy flight is expressed as:

$$\text{Lévy}(\gamma) = 0.01 * \frac{\rho}{\lceil \sigma^{1/\gamma} \rceil}, \tag{10}$$

where ρ and σ are typically distributed and can be selected based on the $\rho \sim N(0, \vartheta_\rho^2)$ and $\sigma \sim N(0, \vartheta_\sigma^2)$, respectively.

The values of ϑ_ρ^2 and ϑ_σ^2 are calculated by:

$$\vartheta_\rho^2 = \left(\frac{\Gamma(1 + \gamma)\sin\left(\frac{\pi\gamma}{2}\right)}{\Gamma\left(\frac{1+\gamma}{2}\right)\gamma 2^{\left(\frac{\gamma-1}{2}\right)}} \right)^{\frac{1}{\gamma}}, \quad \vartheta_\sigma^2 = 1, \tag{11}$$

where $\Gamma(\gamma)$ represents the gamma function, with γ being a constant that affects the trajectory of the Lévy flight step. In this paper, we have selected γ to be 1.5. The mathematical formulation of updating individual positions through the golden

sine strategy guided by the Lévy flight mechanism is illustrated in Eq. (12) from the exploitation phase.

$$X_P(I + 1) = X_P(I)\sin(R_{\text{nd1}}) + \text{Lévy}(\gamma)\sin(R_{\text{nd1}})$$
$$F_{w1}(1 - S)CX_v\Big(X_P(I) - X_P^{\text{flock}}\Big). \tag{12}$$

The proposed HGGOC algorithm initiates by generating a diverse set of individuals randomly, as outlined in Algorithm 1. Each individual presents a potential solution that can be considered as a candidate to address the problem. The HGGOC population is denoted as X_{P_i}, where $i = 1, 2, \ldots, n$, and n represents the number of gaggles. The Dynamic group behavior of the proposed HGGOC algorithm segregates all individuals into an exploration group (G_{n_1}) and an exploitation group (G_{n_2}). The quantity of solutions in each group dynamically adjusts during each iteration based on the best solution. The exploration group involves n_1 agents, while the exploitation group consists of n_2 agents. The proposed HGGOC algorithm initializes the groups with an equal distribution of 50% exploration and 50% exploitation. Subsequently, the number of agents in the exploration group (G_{n_1}) decreases, while the number of agents in the exploitation group (G_{n_2}) increases. However, if the objective function value of the best solution remains unchanged for three consecutive iterations, the algorithm starts increasing the number of agents in the exploration group (G_{n_1}), in order to discover alternative best solutions and prevent potential local optima.

D. Fitness Evaluation

The main objective of the proposed work is to minimize energy consumption in 6G-enabled IoMT networks, thereby fostering sustainable communication within these systems. A crucial element in achieving this is the role of the CH, which is instrumental in managing the network's energy usage. CH is selected through an optimized solution provided by the HGGOC algorithm. We have developed a comprehensive fitness function incorporating various critical parameters to determine the CH effectively. Each of these parameters plays a key role in the CH selection process. This detailed approach ensures an effective strategy for energy management in 6G-enabled IoMT networks. In this work, we incorporated four different fitness parameters, i.e., residual energy, node and sink proximity, remaining energy levels of nodes, and cluster's energy. This multifaceted approach ensures a more comprehensive and efficient selection process.

1) Residual Energy: This fitness parameter is very relevant for the cluster head (CH) because CH consumes more energy than other cluster member nodes due to its role in collecting and transmitting data to the sink. Therefore, choosing a CH with the highest possible energy level is vital. As the network operates, the nodes' energy levels naturally deplete over time, altering their residual energy after each round. To assess this, the first fitness factor is denoted as F_1:

$$F_1 = \sum_{K=1}^{N} \frac{\varepsilon_{\text{resid}}(K)}{\varepsilon_{\text{init}}(K)}, \tag{13}$$

which evaluates the ratio of the node's residual energy (E_{resid}) to its initial energy (E_{init}).

Algorithm 1 HGGOC

Input: Initial population X_{p_i}, where $i = 1, 2, \cdots, n$, n, $I_{\max}$
Output: Best Search Agent as CH

1: **Start Procedure**
2: Initialize the values of $I = 1$, $S_1 = 1$, $\gamma = 1.5$, $\rho = 2$
3: Select values of R_{nd1}, R_{nd2}, R_{nd3}, R_{nd4}, R_{nd5}, F_{w1}, F_{w2}, F_{w3}, F_{w4}
4: Compute the values of CX_{vector} and Aux_{vector}
5: **while** $I \leq I_{\max}$ **do**
6:   **for** $i = 1$ to n **do**
7:     Calculate each search agent's fitness using Eq. (17)
8:     Update the exploration groups (Gn_1) and (Gn_2)
9:   **end for**
10:   **for** $i = 1$ to n_1 **do**
11:     **if** $I \mod 2 == 0$ **then**
12:       **if** $R_{nda} < 0.5$ **then**
13:         **if** $|Aux_v| < 1$ **then**
14:           Modify the present location of the search agent using Eq. (1)
15:         **else**
16:           Select paddling search agents position X_P^{Pdl1}, X_P^{Pdl2}, and X_P^{Pdl3}
17:           Update the value of S using Eq. (3)
18:           Modify the present location of the search agent using Eq. (2)
19:         **end if**
20:       **else**
21:         Modify the present location of the search agent using Eq. (4)
22:       **end if**
23:     **else**
24:       Select search agents position X_P^{sty1}, X_P^{sty2}, and X_P^{sty3}
25:       Lévy Flight with Golden Sine Strategy is applied using Eq. (10)
26:       Update the individual's position using Eq. (12)
27:     **end if**
28:   **end for**
29:   **for** $i = 1$ to n_2 **do**
30:     **if** $I \mod 2 == 0$ **then**
31:       Use Eq. (5), Eq. (6), and Eq. (7) to compute X_{P1}, X_{P2}, and X_{P3}, respectively
32:       Update the individual's position using Eq. (8)
33:     **else**
34:       Select search agents position X_P^{sty1}, X_P^{sty2}, and X_P^{sty3}
35:       Apply Lévy Flight mechanism with Golden Sine Strategy using Eq. (10)
36:       Modify the present location of the search agent using Eq. (12)
37:     **end if**
38:   **end for**
39:   Compute fitness value using Eq. (17)
40:   Update all parameters for the next iteration
41:   $I = I + 1$
42:   Adapt solutions beyond the boundaries of the search space
43:   **if** Pbest is the same as the previous two iterations **then**
44:     Keep posted on solutions within exploration group (G_n) & (G_{n_1})
45:   **end if**
46: **end while**
47: Return best search agent
48: **End procedure**

---

2) Node and Sink Proximity: In this work, the communication distance of sensor nodes, either with other nodes or the sink, is a critical factor. The proximity of a node to the sink is a key consideration, particularly for selecting the CH.

It's preferable to select CH, a node that is closest to the sink, to minimize energy consumption. This fitness parameter evaluates the distance of a candidate node from the sink ($D_{\text{SNode-Sink}}$) relative to the average distance of all nodes from the sink ($D_{\text{Avg(SNodes-Sink)}}$), ensuring energy-efficient operation of the network.

$$F_2 = \sum_{K=1}^{N} \frac{D_{\text{SNode-Sink}}(K)}{D_{\text{Avg(SNodes-Sink)}}(K)}. \tag{14}$$

3) Remaining Energy Levels of Nodes: Once network operation begins, the network's energy starts to deplete, leading to an increase in the number of dead nodes over time. This situation makes the selection of the CH from the remaining active nodes a critical concern. In our approach, we define a fitness parameter, as shown below:

$$F_3 = \frac{1}{N} \sum_{K=1}^{N} \varepsilon_{\text{resid}}(K). \tag{15}$$

which assesses the network's remaining energy. For optimal CH selection, this parameter must remain as high as possible, ensuring that the most energy-efficient nodes are chosen to maintain network functionality and longevity.

4) Cluster's Energy: As nodes within a cluster consume energy, the overall energy level of the cluster decreases. To achieve effective load balancing across the network, the selection of the CH should consider the current energy status of the cluster where the candidate node resides. Initially, this factor is set to 1 in the first round since the cluster formation occurs after the CH is selected. However, from the second round onwards, the energy level of the cluster becomes a significant factor in CH selection. We calculate the fifth fitness parameter, denoted as F_4:

$$F_4 = \sum_{K=1}^{N_{\text{CH}}} \varepsilon_{\text{resid}}(K). \tag{16}$$

It needs to be high to facilitate the selection of a suitable candidate node as CH, thereby ensuring efficient energy management and balanced load distribution within the network.

In our approach, we transform a multi-objective fitness function into a single-objective one by integrating various fitness parameters. As detailed in our methodology, this is achieved by multiplying these parameters with linear weight functions. This integration simplifies the evaluation process while still considering the diverse aspects critical to the system's performance.

$$F = \alpha F_1 + \beta F_2 + \lambda F_3 + \delta F_4, \tag{17}$$

where $\alpha + \beta + \lambda + \delta = 1$. It presents the weighted sum of various factors, each multiplied by corresponding parameters. This approach involves evaluating each node based on its fitness function value. The node that exhibits the highest fitness value through this calculation is then selected as the CH.

E. Complexity

The computational complexity of the proposed HGGOC algorithm can be analyzed in various stages. The initialization

phase involves generating a diverse population, with each individual presenting a potential solution. This initial step incurs a complexity of $\mathcal{O}(n)$, where n is the population size. During each iteration, the algorithm dynamically adjusts the group sizes for exploration and exploitation, contributing to the complexity of $\mathcal{O}(n)$ for each phase. The exploration phase, driven by the movement of search agents based on auxiliary vectors and random parameters, has a complexity of $\mathcal{O}(n)$ due to the necessity of updating each agent's position. The exploitation phase, which refines the solutions through the interaction of multiple agents, adds a complexity of $\mathcal{O}(n^2)$, particularly when computing the new positions based on the behavior of sentries and the Lévy flight mechanism. The fitness evaluation step involves assessing each individual's solution, which also incurs a complexity of $\mathcal{O}(n)$. Given that these steps are repeated for a maximum number of iterations $I_{\max}$, the overall complexity of the algorithm can be expressed as $\mathcal{O}(I_{\max}\cdot n^2)$. This complexity reflects the comprehensive nature of the algorithm, balancing exploration and exploitation while dynamically adjusting the search process to avoid local optima and achieve optimal clustering.

The algorithm needs to maintain a population of n individuals, where each individual represents a potential solution in the search space. Assuming each solution requires m units of space (where m depends on the dimensionality of the problem or the number of variables in the solution), the space required for storing the population is $\mathcal{O}(n\cdot m)$. Therefore, the overall space complexity of the proposed HGGOC algorithm is $\mathcal{O}(n \cdot m)$. This linear space complexity reflects the algorithm's efficient management of resources while handling the optimization process.

V. Blockchain Integration

In the proposed approach blockchain technology is integrated with 6G-enabled IoT environments to significantly enhance data security and integrity [26]. The system model has a core blockchain layer that consists of high computing nodes that form a permissioned blockchain network. This implies that all participating nodes are pre-authenticated and have established trust within the network. The nodes employ a Proof of Authority (PoA) mechanism, which is a lightweight consensus protocol in which a designated set of trusted nodes, known as authorities, validate transactions and generate new blocks. When the cluster heads transmit the data to the core blockchain layer, a blockchain node performs validation, approves the transaction and generates a new block. The new block generated is disseminated to other blockchain nodes in the network, ensuring secure and efficient data management. A block in this blockchain consists of two main parts: the header and the transaction data. The header contains essential information like the block's version, generation timestamp, nonce, difficulty target, Merkle root, and the preceding block's hash. Significantly, the current block's hash incorporates the previous block's hash, ensuring a secure and tamper-evident chain of blocks. Any alteration in a block's content results in a cascading change in the hashes of subsequent blocks.

The validation of each block involves multiple checks. The verifier first ensures the existence and validity of the previous block, and that the current block's timestamp is greater than its predecessor's. Other parameters, such as the transaction root and difficulty, are also verified for validity. Each transaction within the block is individually validated, and any transaction failure leads to an error message. The block is considered validated if all transactions are validated successfully and the final state aligns with the root state. The formula for calculating a block's hash is given by:

$$\text{Hash}(B_n) = \text{Hash}(\text{Hash}(B_{n-1}) + B_{n\text{Data}}), \qquad (18)$$

where B_n represents the block for which the hash is being calculated, $\text{Hash}(B_{n-1})$ is the previous block's hash, and $B_{n\text{Data}}$ denotes the current block data.

Using the hash of the previous block in the current block's hash calculation greatly enhances the blockchain's resistance to attacks. Once a significant number of blocks have been added to the chain, altering data in any block becomes highly impractical. This is because any change would cause a mismatch in the hashes of all subsequent blocks, thereby compromising the integrity of the entire blockchain and effectively securing it against tampering.

In this system, cluster heads aggregate data from IoMT sensor devices, reducing the transaction volume reaching the blockchain and easing the processing load on nodes. A permissioned blockchain using PoA consensus, with a small set of pre-approved validators, enables faster transaction validation, lowers latency, and enhances throughput compared to traditional methods like PoW or PoS. By limiting the number of validator nodes, network congestion and energy consumption are reduced, making the system scalable and efficient for IoT devices.

VI. Performance Evaluation

The performance of the proposed method is rigorously evaluated using essential performance metrics, including stability, network lifetime, remaining network energy, cluster head-count, and throughput analysis. MATLAB has been utilized for these evaluations, adhering to the simulation parameters used in [9], [12], [14]. In the simulations, 100 nodes are randomly deployed in a 100×100 m^2 area with a total energy of 70 Joules for different levels of heterogeneity. In homogeneous networks, each node has 0.7 J energy. In 2-level heterogeneous networks, normal nodes have 0.5 J, and advanced nodes have 1.0 J, with 60 and 40 nodes, respectively. In 3-level heterogeneous networks, normal nodes have 0.5 J, intermediate nodes have 1.0 J, and advanced nodes have 1.5 J, with 50, 30, and 20 nodes, respectively. The details of the energy and node categorization are given in Section III. The performance of the proposed method is benchmarked against several established protocols, including ICITS [8], OptiGA-ASR-DDC [9], OptimizedGA-MS-In&Out-DDC-ASR [12], and OptiGeA-MoMS-In&Out-DDC [14]. This study aims to validate the efficacy and adaptability of the proposed approach in improving the performance of 6G-enabled IoMT networks. Table II shows the key simulation parameters for the network.

TABLE II
NETWORK SIMULATION PARAMETERS

Simulation Parameters	Values
Number of 6G-enabled IoMT devices	100
n_{nrm}, n_{int} & n_{adv} nodes energy	1.0 J, 1.50 J, & 2.0 J
Target area (m^2)	100×100
n_{nr}, n_{in} & n_{ad} node density ratio	70%, 20% & 10% of all nodes
Number of clusters and CN	Dynamic
Sink Location	50×50
d_T	$75m$
Data packet's size	2000 bits
Initial search whales (agents)	50
ω, ψ	2, 1
k, k_0	0.2, 0.3
Initial population Size	50
I_{Max}	40

Fig. 2. Comparative Stability Analysis of Existing and Proposed Methods Across Rounds.

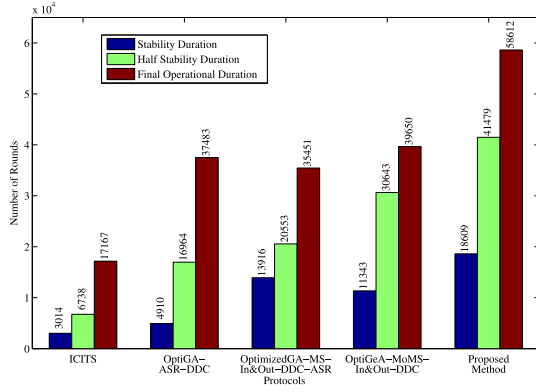Fig. 3. Comparative Analysis of Network Lifetime of Existing and Proposed Methods Across Rounds.

A. Stability Analysis

Fig. 2 illustrates a comparative stability analysis among several existing methods such as ICITS [8], OptiGA-ASR-DDC [9], OptimizedGA-MS-In&Out-DDC-ASR [12], OptiGeA-MoMS-In&Out-DDC [14] and the proposed method, with the analysis conducted over a number of rounds. The existing ICITS method shows a stability period ending 3,014 rounds, while OptiGA-ASR-DDC maintains stability for 4,910 rounds. The OptimizedGA-MS-In&Out-DDC-ASR method achieves a longer stability period of 13,916 rounds, and OptiGeA-MoMS-In&Out-DDC sustains for 11,343 rounds. In stark contrast, the proposed method, HGGOC significantly outstrips these figures, boasting a stability period of 18,609 rounds. This remarkable performance of the proposed method represents substantial improvements in stability periods by 517.41% over ICITS, 279.00% over OptiGA-ASR-DDC, 33.72% over OptimizedGA-MS-In&Out-DDC-ASR, and 64.05% over OptiGeA-MoMS-In&Out-DDC.

B. Network Lifetime Analysis

Fig. 3 presents a comparative analysis focused on the number of active nodes across various rounds, encompassing both established protocols such as ICITS [8], OptiGA-ASR-DDC [9], OptimizedGA-MS-In&Out-DDC-ASR [12], and OptiGeA-MoMS-In&Out-DDC [14] and the proposed method. This comparison is particularly considered in terms of node
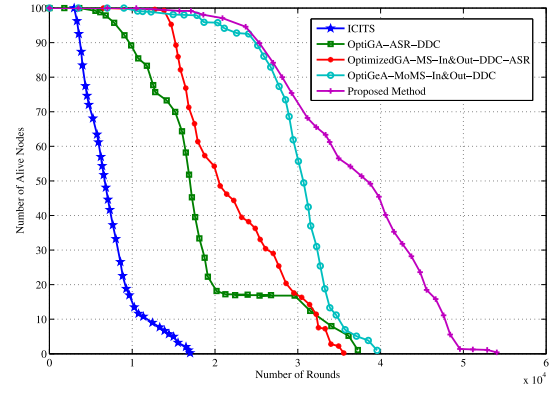
longevity. The proposed method, HGGOC notably outperforms the established ones in maintaining active nodes over time. It shows an increase in node lifetime by 241.42% compared to ICITS, 56.36% over OptiGA-ASR-DDC, 65.33% compared to OptimizedGA-MS-In&Out-DDC-ASR, and 47.82% over OptiGeA-MoMS-In&Out-DDC. This significant improvement in the longevity of active nodes is primarily due to the optimized detection range incorporated in our protocol. The optimized distance plays a pivotal role in the formation of smaller clusters. This strategic formation effectively reduces the load on individual sensor nodes, thereby conserving energy. This aspect is especially beneficial for cluster heads located closer to the sink, as it lessens their energy expenditure. Consequently, the protocol enhances the overall energy efficiency and extends the operational lifespan of the network nodes, an essential factor for the sustainability and effectiveness of IoMT networks.

C. Network Remaining Energy Analysis

Fig. 4 provides a detailed depiction of the energy consumption metrics across different rounds within the IoMT sensor system. This system begins to expend energy as soon as information transmission is initiated, making it essential to track the behavior of the system's remaining energy after this transmission begins. As demonstrated in the figure, the proposed protocol shows a marked improvement over existing protocols like ICITS [8], OptiGA-ASR-DDC [9], OptimizedGA-MS-In&Out-DDC-ASR [12], and OptiGeA-MoMS-In&Out-DDC [14] in terms of sustaining energy for the maximum number of network activity rounds. This enhanced performance can be attributed to advancements in managing the distance factor, achieved through the strategic use of multiple sinks. This setup significantly reduces the energy required for data transmission. The protocol effectively minimizes energy drain by distributing the energy load more evenly, particularly on the cluster heads. The deployment of a single sink at the center of the target region plays a crucial role in enhancing efficiency. This sink is strategically positioned to gather information from cluster heads located across the network. These sinks are positioned to gather information from cluster heads across the network, even those sparsely situated.
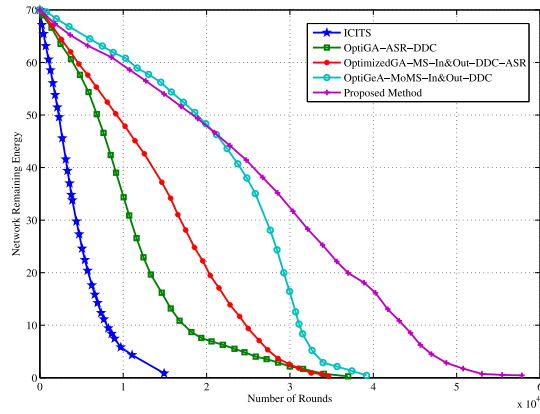
Fig. 4. Comparative Analysis of Residual Energy of Existing and Proposed Methods Across Rounds.
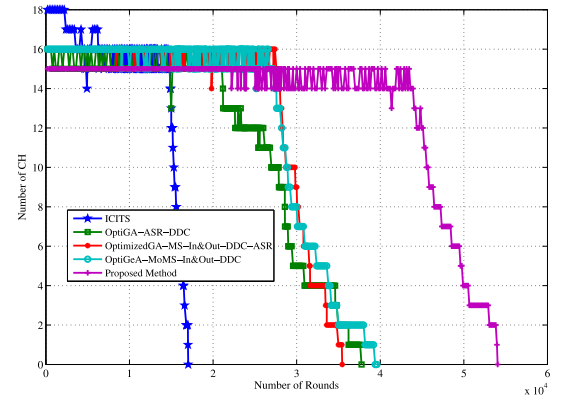

Fig. 5. Comparative Analysis of Cluster Head Count per Round for Existing and Proposed Methods.

Fig. 6. Comparative Analysis of Packets Sent to Sink per Round for Existing and Proposed Methods.

This arrangement prevents data packets from traveling long distances, conserving a considerable amount of energy. This approach represents a significant leap in enhancing the sustainability and effectiveness of sensor networks, particularly in scenarios requiring prolonged operation and high energy efficiency.

D. Cluster Head Count Analysis

Fig. 5 vividly illustrates the dynamics of cluster headcount over various rounds, highlighting the influence of the fittest SN based on the efficient fitness evaluation process on cluster formation over the operational period. The protocol is designed to maintain an optimal number of cluster heads, which are generated through the proposed HGGOC approach. This optimal number of CHs is a key metric in ensuring the efficient structuring of clusters as determined by the fittest SN. Initially, the protocol starts with moving towards the optimal solution. As the process evolves, it progressively moves towards a more efficient structural arrangement. This involves strategically positioning the most relevant cluster heads based on their appropriateness fitness values The network begins its operation with this initially evolved clustering configuration and continues functioning until the stability period is reached, which is indicated by the depletion of the first node. As the network's energy gradually depletes, the selection process adapts, seeking to prolong the network's overall lifetime by adjusting the cluster head nodes.

In the early stages of operation, we observe that existing methods display a wide range of cluster head counts, from 18 to 0, with a sharp decrease. However, the proposed protocol manages to maintain a more consistent cluster headcount, typically ranging from 15 to 14. This difference is primarily due to the elimination of unnecessary cluster formations, especially those near the base stations. Moreover, this cluster headcount metric also sheds light on the functionality of the optimization process in the protocol. It illustrates how the cluster head count dynamically adjusts based on factors such as node fitness and remaining energy levels. As the operation of the system progresses, the cluster head count demonstrates a gradual decrease, reflecting the ongoing optimization process within
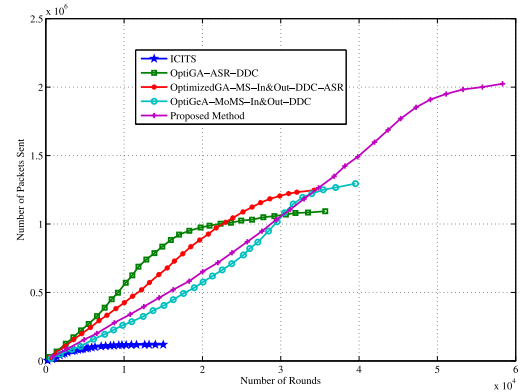
the network. This dynamic adjustment is key to maintaining the efficiency and longevity of the network.

E. Throughput Analysis

In the network design, minimizing cluster structuring near the base station and optimizing the transmission distance factor have led to a notable improvement in the network's quality of service (QoS). The four key fitness parameters used for determining cluster heads collectively enhance the network's lifespan and increase its throughput. The capacity to transmit a higher volume of data packets is directly linked to the prolonged operational duration of the 6G-enabled IoMT devices. Fig. 6 depicts the number of data packets sent over various rounds, highlighting a significant improvement in both throughput and lifespan with our proposed method. Specifically, our approach achieves the transmission of 2.02 million packets, a substantial increase compared to the 0.11 million, 1.08 million, 1.24 million, and 1.27 million packets transmitted by existing methods. One of the key advantages of the proposed approach is the significant energy savings realized by independent 6G-enabled IoMT devices. By minimizing unnecessary traffic near the base station, the strategy conserves energy, which is then translated into increased throughput. This demonstrates the effectiveness of our method in enhancing network efficiency and sustainability.

VII. CONCLUSION AND FUTURE WORK

In this paper, we concentrated on advancing secure and sustainable communication, specifically focusing on energy-efficient communication for 6G-enabled IoMT devices. To address this, we introduced a novel HGGOC algorithm and developed a fitness function specifically tailored for CH selection. By leveraging the robust features of blockchain, our approach ensures secure and transparent data management across expansive 6G-enabled IoMT networks. This integration mitigates potential vulnerabilities and establishes a solid foundation for accountable and auditable network operations. The effectiveness of the proposed work was evaluated using several key metrics designed to verify the protocol's efficiency and performance. The findings from these evaluations have been quite promising, particularly in terms of enhancing the network lifespans of 6G-enabled IoMT devices. This improvement is significant as it contributes directly to the sustainability and effectiveness of IoMT networks in a 6G environment.

Future work will focus on addressing the mobility aspects of IoMT devices, motivated by the expectation that 6G systems will support higher mobility. Additionally, we will explore the scalability of the HGGOC algorithm in large-scale IoMT deployments, including heterogeneous networks with diverse device types and varying energy profiles. The impact of different security concerns and blockchain configurations on network performance and energy consumption could also be examined.

REFERENCES

[1] S. R. Pokhrel, S. Verma, S. Garg, A. K. Sharma, and J. Choi, "An efficient clustering framework for massive sensor networking in industrial Internet of Things," *IEEE Trans. Ind. Informat.*, vol. 17, no. 7, pp. 4917–4924, Jul. 2021.

[2] Y. Chen, Z. Ren, J. Xu, Y. Zeng, D. W. K. Ng, and S. Cui, "Integrated sensing, communication, and powering (ISCAP): Towards multi-functional 6G wireless networks," 2024, *arXiv:2401.03516*.

[3] A. Mukherjee, D. De, N. Dey, R. G. Crespo, and E. Herrera-Viedma, "DisastDrone: A disaster aware consumer Internet of Drone Things system in ultra-low latent 6G network," *IEEE Trans. Consum. Electron.*, vol. 69, no. 1, pp. 38–48, Feb. 2023.

[4] K. B. Letaief, W. Chen, Y. Shi, J. Zhang, and Y.-J. A. Zhang, "The roadmap to 6G: AI empowered wireless networks," *IEEE Commun. Mag.*, vol. 57, no. 8, pp. 84–90, Aug. 2019.

[5] X. Chen, P. Wang, Y. Yang, and M. Liu, "Resource-constraint deep forest-based intrusion detection method in Internet of Things for consumer electronic," *IEEE Trans. Consum. Electron.*, vol. 70, no. 2, pp. 4976–4987, May 2024.

[6] J. K. Samriya, S. Kumar, M. Kumar, M. Xu, H. Wu, and S. S. Gill, "Blockchain and reinforcement neural network for trusted cloud-enabled IoT network," *IEEE Trans. Consum. Electron.*, vol. 70, no. 1, pp. 2311–2322, Feb. 2024.

[7] S. S. Gill and R. Buyya, "Transforming research with quantum computing," *J. Econ. Technol.*, vol. 3, pp. 1–10, Jul. 2024.

[8] S. Verma, S. Zeadally, S. Kaur, and A. K. Sharma, "Intelligent and secure clustering in wireless sensor network (WSN)-based intelligent transportation systems," *IEEE Trans. Intell. Transp. Syst.*, vol. 23, no. 8, pp. 13473–13481, Aug. 2022.

[9] S. Singh, A. S. Nandan, G. Sikka, A. Malik, and N. Kumar, "A genetic-algorithm-based dynamic transmission of data for communicable disease in IoMT environment," *IEEE Internet Things J.*, vol. 11, no. 1, pp. 1427–1438, Jan. 2024.

[10] S. P. Singh, P. Singh, D. Koundal, and M. Diwakar, "A new multi/many-objective optimization approach in wireless sensor networks for e-commerce applications," *IEEE Trans. Consum. Electron.*, vol. 70, no. 2, pp. 4848–4857, May 2024.

[11] P. Prabaharan, "Enhanced energy proficient clustering (EEPC) algorithm for minimizes the energy depletion in wireless sensor network," *J. Intell. Fuzzy Syst.*, vol. 46, pp. 1995–2008, Jan. 2024.

[12] A. S. Nandan, S. Singh, A. Malik, and R. Kumar, "A green data collection & transmission method for IoT-based WSN in disaster management," *IEEE Sensors J.*, vol. 21, no. 22, pp. 25912–25921, Nov. 2021.

[13] D. Gupta et al., "Optimizing cluster head selection for e-commerce-enabled wireless sensor networks," *IEEE Trans. Consum. Electron.*, vol. 70, no. 1, pp. 1640–1647, Feb. 2024.

[14] S. Singh, A. S. Nandan, G. Sikka, A. Malik, and A. Vidyarthi, "A secure energy-efficient routing protocol for disease data transmission using IoMT," *Comput. Elect. Eng.*, vol. 101, Jul. 2022, Art. no. 108113.

[15] B. M. Sahoo, T. Amgoth, and H. M. Pandey, "Particle swarm optimization based energy efficient clustering and sink mobility in heterogeneous wireless sensor network," *Ad Hoc Netw.*, vol. 106, Sep. 2020, Art. no. 102237.

[16] T. A. Alghamdi, "Energy efficient protocol in wireless sensor network: Optimized cluster head selection model," *Telecommun. Syst.*, vol. 74, no. 3, pp. 331–345, 2020.

[17] V. Prakash, D. Singh, S. Pandey, S. Singh, and P. K. Singh, "Energy-optimization route and cluster head selection using M-PSO and GA in wireless sensor networks," *Wireless Pers. Commun.*, pp. 1–26, May 2024. [Online]. Available: https://doi.org/10.1007/s11277-024-11096-1

[18] W. Osamy, B. Alwasel, A. Salim, A. M. Khedr, and A. Aziz, "LBAS: Load-balancing aware clustering scheme for IoT-based heterogeneous wireless sensor networks," *IEEE Sensors J.*, vol. 24, no. 9, pp. 15472–15490, May 2024.

[19] D. Loganathan, M. Balasubramani, R. Sabitha, and S. Karthik, "Improved load-balanced clustering for energy-aware routing (ILBC-EAR) in WSNs," *Comput. Syst. Sci. Eng.*, vol. 44, no. 1, pp. 100–112, 2023.

[20] I. B. Prasad, Yogita, S. S. Yadav, N. Kumar, and V. Pal, "BAT: Barabasi–Albert with Topsis scale-free topology evolution for load-balanced WSNs," *IEEE Sensors J.*, vol. 23, no. 15, pp. 17627–17637, Aug. 2023.

[21] H. Ali, U. U. Tariq, M. Hussain, L. Lu, J. Panneerselvam, and X. Zhai, "ARSH-FATI: A novel metaheuristic for cluster head selection in wireless sensor networks," *IEEE Syst. J.*, vol. 15, no. 2, pp. 2386–2397, Jun. 2021.

[22] T. M. Behera, S. K. Mohapatra, U. C. Samal, M. S. Khan, M. Daneshmand, and A. H. Gandomi, "Residual energy-based cluster-head selection in WSNs for IoT application," *IEEE Internet Things J.*, vol. 6, no. 3, pp. 5132–5139, Jun. 2019.

[23] M. Shahid et al., "Link-quality-based energy-efficient routing protocol for WSN in IoT," *IEEE Trans. Consum. Electron.*, vol. 70, no. 1, pp. 4645–4653, Feb. 2024.

[24] E.-S. M. El-kenawy, N. Khodadadi, S. Mirjalili, A. A. Abdelhamid, M. M. Eid, and A. Ibrahim, "Greylag goose optimization: Nature-inspired optimization algorithm," *Expert Syst. Appl.*, vol. 238, Mar. 2024, Art. no. 122147.

[25] W. Xie, J.-S. Wang, and Y. Tao, "Improved black hole algorithm based on golden sine operator and Levy flight operator," *IEEE Access*, vol. 7, pp. 161459–161486, 2019.

[26] L. K. Ramasamy, K. P. F. Khan, A. L. Imoize, J. O. Ogbebor, S. Kadry, and S. Rho, "Blockchain-based wireless sensor networks for malicious node detection: A survey," *IEEE Access*, vol. 9, pp. 128765–128785, 2021.